3-9-2015

Hybrid Type-I InAs/GaAs and Type-II GaSb/GaAs Quantum Dot Structure with Enhanced Photoluminescence

Hai-Ming Ji
University of California Los Angeles

Baolai Liang
University of California Los Angeles

Paul J. Simmonds
University of California Los Angeles

Bor-Chau Juang
University of California Los Angeles

Tao Yang
Chinese Academy of Sciences

See next page for additional authors

Hybrid type-I InAs/GaAs and type-II GaSb/GaAs quantum dot structure with enhanced photoluminescence

Hai-Ming Ji,[1,2] Baolai Liang,[3,a)] Paul J. Simmonds,[3] Bor-Chau Juang,[1] Tao Yang,[2] Robert J. Young,[4] and Diana L. Huffaker[1,3]
[1]*Department of Electrical Engineering, University of California Los Angeles, Los Angeles, California 90095, USA*
[2]*Institute of Semiconductors, Chinese Academy of Sciences, Beijing 100083, China*
[3]*California NanoSystems Institute, University of California Los Angeles, Los Angeles, California 90095, USA*
[4]*Department of Physics, Lancaster University, Lancaster LA1 4YB, United Kingdom*

(Received 10 December 2014; accepted 3 March 2015; published online 11 March 2015)

We investigate the photoluminescence (PL) properties of a hybrid type-I InAs/GaAs and type-II GaSb/GaAs quantum dot (QD) structure grown in a GaAs matrix by molecular beam epitaxy. This hybrid QD structure exhibits more intense PL with a broader spectral range, compared with control samples that contain only InAs or GaSb QDs. This enhanced PL performance is attributed to additional electron and hole injection from the type-I InAs QDs into the adjacent type-II GaSb QDs. We confirm this mechanism using time-resolved and power-dependent PL. These hybrid QD structures show potential for high efficiency QD solar cell applications. © *2015 AIP Publishing LLC*. [http://dx.doi.org/10.1063/1.4914895]

Semiconductor quantum dots (QDs) have provoked tremendous research interest due to their unique characteristics that stem from three dimensional quantum confinement.[1] In particular, type-I InAs/GaAs QDs have achieved great success and have been adopted widely as the active region material in various optoelectronic devices. Taking one example, InAs/GaAs QDs can be used to extend the absorption range of GaAs-based solar cells and increase their short-circuit current.[2] InAs/GaAs QD solar cells with one-sun efficiencies as high as 18.7% have been demonstrated.[3] However, due to their short interband recombination time, type-I QDs themselves can act as recombination centers deteriorating solar cell performance.[4] As a result, it is not easy to achieve InAs/GaAs QD solar cells with efficiencies exceeding that of a GaAs reference cell.[5] In recent years, type-II QDs have also gained attention because of characteristics arising from their specific band alignment.[6,7] The spatial separation of electrons and holes in type-II QDs reduces spontaneous recombination. Together with their broad spectral response, this property means that GaSb/GaAs QDs[8] and InAs/AlAsSb/InP QDs[9] are being investigated as highly promising active region materials in QD solar cells. However, the spatial separation of electrons and holes also reduces the photon absorption efficiency of type-II QDs compared with type-I InAs QDs. It is, thus, difficult for type-II QD solar cells to compete with type-I InAs/GaAs QD solar cells. Taking into account these drawbacks of both type-I and type-II QDs, it appears that using a single QD nanomaterial may not be the best way to improve the efficiency of solar cells.

Recently, we combined type-II GaSb/GaAs QDs with a type-I InGaAs quantum well (QW) in the fabrication of a QD solar cell.[10] As a complement to the GaSb QDs, the InGaAs QW provides additional absorption beyond the GaAs band edge, helping to enhance infrared photoresponse. However, since InAs/GaAs QDs possess a longer emission wavelength and wider spectral response than InGaAs, they can be used to substitute for the QW and further extend the absorption range of the type-II GaSb/GaAs QD solar cell. In other words, we postulate that GaSb/GaAs QDs could be an excellent addition to the InAs/GaAs QD solar cell.

Suzuki and Arakawa studied the optical properties of coupled InAs/GaAs QDs and GaSb/GaAs QDs in 1999.[11] However, the photoluminescence (PL) signal from their GaSb QDs was found to be weak and it is difficult to see any optical improvement from their measurements. Hospodková *et al*. investigated vertically correlated type-I InAs QDs and type-II GaAsSb QDs separated by a GaAsSb barrier. By changing the Sb composition and size of the GaAsSb QDs, the band alignment could be tuned.[12] Again, there was no definitive evidence of optical improvement due to interaction between the two types of QDs.

In this letter, we report a hybrid type-I InAs/GaAs and type-II GaSb/GaAs QD structure that exhibits a clear enhancement in optical performance. With a thin (5 nm) GaAs spacer layer between the InAs and GaSb QDs, the hybrid structure shows more intense PL with broader spectral range, compared to either InAs or GaSb QD control samples. Using time-resolved and power-dependent PL, we demonstrate that this improvement is due to additional electron and hole injection from the InAs QDs into the adjacent GaSb QDs.

The samples in this study are grown in a Veeco GEN930 solid-source molecular beam epitaxy system equipped with As and Sb crackers. Figure 1(a) shows the schematic diagram of the hybrid QD structure. After thermally removing the native oxidation layer, a 200 nm GaAs buffer layer is first deposited on a semi-insulating GaAs(001) substrate at 580 °C. The substrate is then cooled to 520 °C for the growth of InAs QDs. 2.3 monolayers (ML) of InAs is deposited at 0.018 ML/s with a V/III beam equivalent pressure (BEP) ratio of ∼200 to form the QDs. A 5-nm-thick GaAs spacer layer is used to cap the InAs QDs. Afterwards, the substrate is heated up to

[a)]Author to whom correspondence should be addressed. Electronic mail: bliang@cnsi.ucla.edu

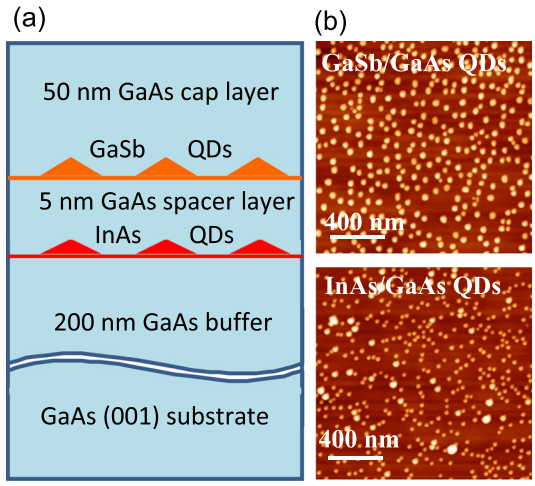

FIG. 1. (a) Schematic diagram of hybrid InAs/GaAs and GaSb/GaAs QD structure. (b) Atomic force microscope images of surface GaSb/GaAs QDs and InAs /GaAs QDs grown for control samples.

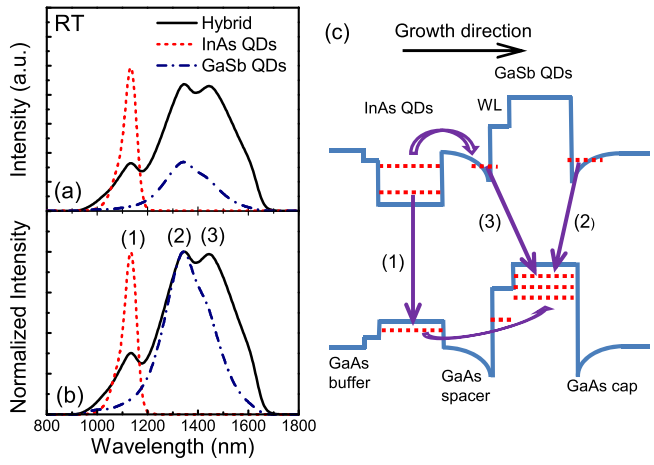

FIG. 2. (a) Room temperature PL spectra of the hybrid QD, InAs QD control, and GaSb QD control samples; (b) PL spectra in (a) normalized to their maximum intensities; and (c) schematic diagram of the band structure for the hybrid QD structure and different radiative recombination routes. Recombination routes (1)–(3) correspond to the peak labels in (b). Solid (hollow) arrows indicate the carrier recombination (injection) processes.

580 °C for 5 min of thermal annealing to smooth the GaAs surface, and then the sample is cooled to 490 °C in preparation for growth of the GaSb QDs. 3.4 ML GaSb is deposited at 0.2 ML/s with a V/III BEP ratio of ~1 to form the GaSb QDs. A 50 nm GaAs capping layer completes the sample. The formation of both InAs and GaSb QDs is confirmed during growth by the RHEED pattern transition from streaky to spotty, as expected. For comparison, control samples containing only InAs QDs or only GaSb QDs are grown with the same growth parameters used for the hybrid QD sample, including the 50 nm GaAs cap layer. The control samples contain one buried QD layer for PL and one surface QD layer for morphology investigation. Atomic force microscopy is performed on the surface InAs and GaSb QDs, as shown in Fig. 1(b). The InAs QDs have an areal density of $1.0 \times 10^{10}\,\mathrm{cm}^{-2}$ and are ~11 nm tall and ~50 nm in diameter, while the GaSb QDs have an areal density of $0.9 \times 10^{10}\,\mathrm{cm}^{-2}$ and are ~15 nm tall and ~70 nm in diameter.

Room temperature (RT) PL measurements on all the samples are performed via a standard lock-in technique using a monochromator, a 532 nm diode pumped solid state laser, and an InGaAs photomultiplier tube (PMT) detector with a spectral response from 950 nm to 1700 nm. Figure 2(a) shows the as-measured RT PL spectra under 100% output pumping power (~150 W/cm^2). In order to compare the peak positions effectively, we have normalized the PL intensity as shown in Figure 2(b). The hybrid QD sample has three peaks (centered at 1135 nm, 1345 nm, and 1445 nm), while the InAs QD and GaSb QD control samples show only one clear peak each. We can assign the 1135 nm PL peak from the hybrid QD sample to emission from InAs QDs, since the InAs QD control sample has a peak in the same position. Similarly, the 1345 nm peak correlates well with the peak position of the GaSb QD control sample. The 1445 nm peak in the hybrid QD structure bears some similarities with the small, long-wavelength shoulder on the peak from the GaSb QD control sample. These three features combine to give the hybrid structure a significantly broader spectrum than either the GaSb or InAs QD control samples. The full width at half maximum (FWHM) of the hybrid QD structure is 343 nm (217 meV), in comparison to 215 nm (145 meV) for the GaSb and 61 nm (58 meV) for the InAs QD control samples, respectively. The spectrum of the hybrid QD structure extends from 920 nm to 1710 nm and may even extend to longer wavelengths, considering the detector's cut-off at 1700 nm. For the hybrid QD sample, the peak intensity at 1135 nm is only one third that for the InAs QD control sample, though the peaks at 1345 nm and 1445 nm are comparable in intensity to the emission from the InAs QD control sample. The integrated PL intensity of the hybrid QD sample is 4.1 times higher than the GaSb QD sample and 4.6 times higher than the InAs QD sample, respectively.

To aid further discussion, the 1135 nm, 1345 nm, and 1445 nm peaks in the hybrid QD sample spectrum in Fig. 2(b) are labeled (1), (2), and (3), respectively. In order to understand the physical processes underlying these peaks in the PL, a schematic diagram of the hybrid QD sample's band structure and recombination routes is shown in Fig. 2(c). Labeling of the recombination routes in Fig. 2(c) is consistent with the peak positions in Fig. 2(b). In the type-II GaSb/GaAs QD structure, electrons are confined in the triangular QW formed on each side of the QDs due to the bending of GaAs conduction band at the GaSb/GaAs interface.[13,14] Both peaks (2) and (3) derive from radiative recombination between electrons confined in these triangular QWs and holes in the GaSb QDs. However, the difference is that the electrons contributing to peak (3) are confined at the interface between the GaSb wetting layer (WL) and GaAs spacer layer (recombination route (3) in Fig. 2(c)); the electrons contributing to peak (2) are confined at the interface between the GaSb QDs and GaAs cap layer (recombination route (2) in Fig. 2(c)). This conclusion is based on the following evidence:

(i) The confinement of electrons on the WL side is slightly weaker because of the lower potential barrier of the WL. Thus, recombination route (3) should correspond to PL emission at a longer wavelength.

(ii) The wavelength of peak (2) is the same in the GaSb QD control and hybrid QD samples. This peak, thus, arises from electrons confined in the triangular QW at the interface between the GaSb QDs and GaAs cap, since the band structure here will be least affected by the addition of the InAs QDs.

(iii) For the GaSb QD control sample, PL intensity at wavelength position (3) is only 60% of the intensity of peak (2). Relatively small overlap between the electron and hole wavefunctions on the WL side of the control QDs leads to reduced PL intensity at wavelength position (3) in the PL spectrum with sufficient carrier injection.

Peak (1) is related to inter-band recombination in the InAs QDs. It should be noted that peak (1) from the hybrid structure is broader than that from the InAs QD control sample. This broadening is attributed to radiative recombination between electrons in the triangular QW on the GaSb WL side and holes confined in the GaSb WL at a similar energy, which is much more dominant below 200 K (data not shown here).

In the hybrid QD structure, additional electrons are injected from InAs QDs to the adjacent triangular QW on the WL side (see curved hollow arrow in Fig. 2(c)), while the holes are injected from the InAs QDs to the GaSb QDs (hollow arrow in Fig. 2(c)) by tunneling through the 5 nm GaAs spacer. In addition, the WLs can be regarded as reservoirs of carriers for the QDs. Since the distance between the InAs WL and the GaSb WL is only 5 nm, it is possible that some of the carriers can be injected into the GaSb QDs through the GaSb WL. The electron and hole injection strengthen recombination route (3) and results in peak (3) having almost the same intensity as peak (2). PL intensities of peaks (2) and (3) in the hybrid structure are 2.6 and 4.0 times higher, respectively, than in the GaSb QD control sample. As noted above, the intensity of peak (1) in the hybrid structure is only ~33% of the signal from the InAs QD control sample, which is consistent with the loss of carriers in the InAs QDs via injection into the GaSb QDs. To summarize this section, we conclude that in the hybrid QD structure the PL performance of the GaSb QDs is significantly improved at the expense of PL performance of the InAs QDs.

Time-resolved PL (TRPL) measurements are performed on the hybrid QD and GaSb QD control samples at room temperature using time-correlated single-photon counting,[15] as shown in Fig. 3. The signal is excited by a 650 nm laser pulse (~20 ps pulse width) from a supercontinuum laser operating at a 15.6 MHz repetition rate. The decay curves are labeled (2) and (3) in accordance with peak positions (2) and (3) in Fig. 2(b) as well as recombination routes (2) and (3) in Fig. 2(c). A double exponential decay model $I(t) = A_1 \exp(-t/\tau_1) + A_2 \exp(-t/\tau_2)$ is employed to fit the TRPL curves in which A_1 (A_2) is the amplitude and τ_1 (τ_2) is the decay time constant for the slow (fast) decay process. τ_{av} is the intensity weighted average lifetime and w_1 (w_2) is the weight of τ_1 (τ_2). The inset table in Fig. 3 shows the fitting results.

As mentioned above, decay curve (3) stems from electrons confined in the triangular QW on the WL side, while decay curve (2) comes from electrons confined on the other

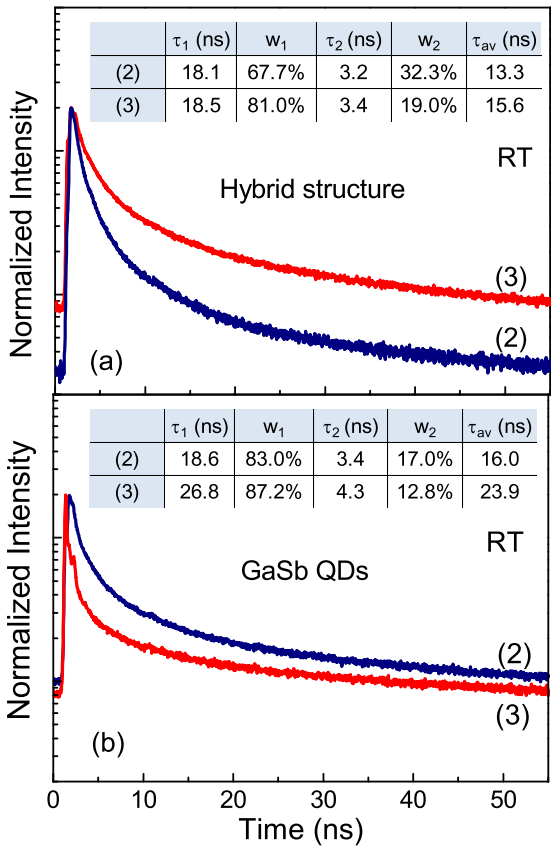

	τ_1 (ns)	w_1	τ_2 (ns)	w_2	τ_{av} (ns)
(2)	18.1	67.7%	3.2	32.3%	13.3
(3)	18.5	81.0%	3.4	19.0%	15.6

	τ_1 (ns)	w_1	τ_2 (ns)	w_2	τ_{av} (ns)
(2)	18.6	83.0%	3.4	17.0%	16.0
(3)	26.8	87.2%	4.3	12.8%	23.9

FIG. 3. Room temperature time-resolved PL of (a) hybrid QD sample and (b) GaSb QD sample. The decay curves are labeled (2) and (3) in accordance with peak positions (2) and (3) in Fig. 2(b) as well as recombination routes (2) and (3) in Fig. 2(c). The inset table shows the fitting results based on a double exponential decay model. τ_1 (τ_2) is the decay time for the slow (fast) decay process. τ_{av} is the intensity weighted average lifetime and w_1 (w_2) is the weight of τ_1 (τ_2).

side of the GaSb QDs. For the GaSb QD control sample, recombination route (2) has a τ_1 of 18.6 ns and a τ_2 of 3.4 ns, while recombination route (3) has a τ_1 of 26.8 ns and a τ_2 of 4.3 ns. τ_2 (fast decay process) is related to radiative recombination while τ_1 (slow decay process) is related to carrier recapture.[16,17] Due to the weak electron-hole overlap on the GaSb WL side, both the slow and the fast decay processes of recombination route (3) are slower than those of recombination route (2). This helps to explain the lower PL intensity of peak (3) compared with peak (2) for the GaSb QD control sample in Fig. 2(a). For the hybrid QD sample, extra hole injection from adjacent InAs QDs to the GaSb QDs leads to an increased w_2 (from 17.0% to 32.3%) for recombination route (2) and a decreased τ_2 (from 4.3 ns to 3.4 ns) for recombination route (3). This agrees with the large enhancement in PL intensity exhibited by the hybrid QD sample. Also, due to the electron injection from InAs QDs, the electron recapture (refill) process in the triangular QW on the GaSb WL side is accelerated. As a result, τ_1 for recombination route (3) undergoes a decrease from the GaSb QD control sample (26.8 ns) to the hybrid QD sample (18.5 ns).

In order to investigate the optical performance of the hybrid QD structure under different carrier injection levels, the output pumping power is decreased from 100% to 1%. Figure 4 shows normalized room temperature power-dependent PL spectra for the hybrid QD and GaSb QD

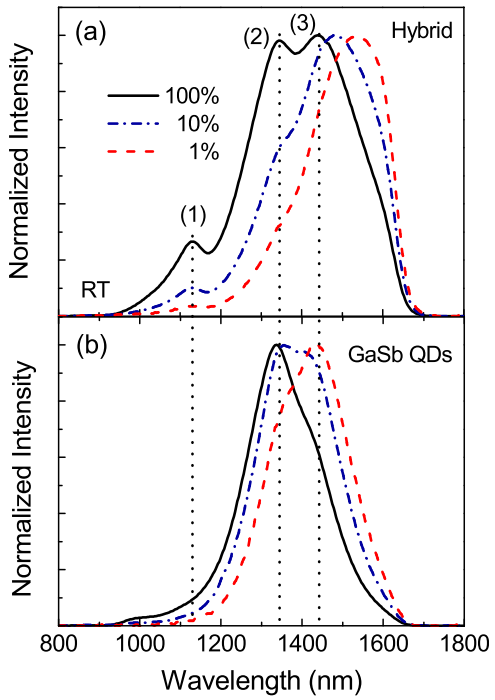

FIG. 4. Normalized room temperature power-dependent PL of (a) hybrid QD sample and (b) GaSb QD control sample. Peak positions (1)–(3) for hybrid QD sample correspond to the recombination routes (1)–(3) in Fig. 2(c).

control samples. Peak positions (1)–(3) correspond to recombination routes (1)–(3) in Fig. 2(c). For the hybrid QD structure (Fig. 4(a)), recombination route (3) has much brighter PL under both 1% and 10% pumping powers and similar intensity to recombination route (2) even under 100% pumping power. This is a result of the faster recombination rate of route (3) due to the extra carrier injection from InAs QDs to GaSb QDs. For the GaSb QD sample (Fig. 4(b)), recombination route (2) dominates under 100% pumping power while recombination route (3) dominates under 1% pumping power. For an intermediate 10% pumping power, recombination routes (2) and (3) have almost the same PL intensity. This is because at low pumping power, electrons preferentially occupy the lower energy levels in the triangular QW on the WL side and so recombine via route (3). At high pumping power both triangular QWs are readily filled, but due to the lower recombination rate of route (3), most carriers combine via route (2). At intermediate (10%) pumping power, higher electron density in the triangular QW on the WL side compensates the lower recombination rate of route (3), leading to nearly the same PL intensity for routes (2) and (3). We also observe a large red-shift of the longest wavelength peak in the hybrid QD structure as the pumping power is decreased. However, this cannot be fully explained by the well-known blue-shift in type-II GaSb/GaAs QDs that is proportional to the cube root of the excitation density.[14,18,19] We believe that an indirect radiative recombination process exists between electrons confined in InAs QDs and holes confined in GaSb QDs. This indirect process has a longer PL wavelength and is more obvious under low pumping power at low temperature due to its slower recombination rate (data not shown here).

In recent years, the use of built-in charge from doping InAs/GaAs QDs has been demonstrated as an efficient way to improve solar cell performance.[20–22] In the hybrid type-I InAs/type-II GaSb QD structure presented in this letter, the extra injection of carriers from the InAs QDs can be regarded as providing a special kind of built-in charge in the GaSb QDs. This process can simultaneously be thought of as hole (electron) injection to the conduction (valence) band of the InAs QDs. As a result, inter-band light absorption could be enhanced and inter-band carrier recombination could be inhibited in the InAs QDs. Furthermore, intra-band light absorption could be strengthened in the GaSb QDs. This hybrid type-I and type-II QD structure hence shows great potential for improving the efficiency of QD solar cells.

In summary, we have investigated the PL properties of a hybrid InAs/GaAs and GaSb/GaAs QD structure. The hybrid QD structure exhibits a clear enhancement in optical performance, which we have demonstrated derives from electron and hole injection from the type-I InAs QDs into the type-II GaSb QDs. As a result, this hybrid QD structure shows promise for creating high efficiency QD solar cells.

The authors gratefully acknowledge the financial support of United States Department of Defense (NSSEFF N00244-09-1-0091) and the University of California Lab Fees Research Program (Grant No. 12-LR-238568). H. M. Ji and T. Yang acknowledge support from CAS-UCLA Training Program and National Science Foundation of China (Nos. 61204057 and 91433206). R. J. Young acknowledges support by the Royal Society through a University Research Fellowship (UF110555).

[1]D. Bimberg, M. Grundmann, and N. N. Ledentsov, *Quantum Dot Heterostructures* (Wiley, 1999).
[2]A. Luque, A. Marti, N. Lopez, E. Antolin, and E. Canovas, Appl. Phys. Lett. **87**, 083505 (2005).
[3]K. Tanabe, D. Guimard, D. Bordel, and Y. Arakawa, Appl. Phys. Lett. **100**, 193905 (2012).
[4]F. Xu, X. G. Yang, S. Luo, Z. R. Lv, and T. Yang, J. Appl. Phys. **116**, 133102 (2014).
[5]Y. X. Gu, X. G. Yang, H. M. Ji, P. F. Xu, and T. Yang, Appl. Phys. Lett. **101**, 081118 (2012).
[6]F. Hatami, N. N. Ledentsov, M. Grundmann, J. Bohrer, F. Heinrichsdorff, M. Beer, D. Bimberg, S. S. Ruvimov, P. Wemer, U. Gosele, J. Heydenreich, U. Richter, S. V. Ivanov, B. Ya. Meltser, P. S. Koper, and Zh. I. Alferov, Appl. Phys. Lett. **67**, 656 (1995).
[7]M. Geller, C. Kapteyn, L. Muller-Kirsch, R. Heitz, and D. Bimberg, Appl. Phys. Lett. **82**, 2706 (2003).
[8]R. B. Laghumavarapu, A. Moscho, A. Khoshakhlagh, M. El-Emawy, L. F. Lester, and D. L. Huffaker, Appl. Phys. Lett. **90**, 173125 (2007).
[9]P. J. Simmonds, R. B. Laghumavarapu, M. Sun, A. Lin, C. J. Reyner, B. Liang, and D. L. Huffaker, Appl. Phys. Lett. **100**, 243108 (2012).
[10]R. B. Laghumavarapu, B. L. Liang, Z. S. Bittner, T. S. Navruz, S. M. Hubbard, A. Norman, and D. L. Huffaker, Sol. Energy Mater. Sol. Cells **114**, 165 (2013).
[11]K. Suzuki and Y. Arakawa, in *Quantum Optoelectronics, OSA Technical Digest* (Optical Society of America, 1999), Paper No. QMC2.
[12]A. Hospodková, J. Oswald, J. Pangrác, M. Zíková, J. Kubištová, Ph. Komninou, J. Kioseoglou, K. Kuldová, and E. Hulicius, J. Appl. Phys. **114**, 174305 (2013).
[13]E. R. Glaser, B. R. Bennett, B. V. Shanabrook, and R. Magno, Appl. Phys. Lett. **68**, 3614 (1996).
[14]D. Alonso-Álvarez, B. Alén, J. M. García, and J. M. Ripalda, Appl. Phys. Lett. **91**, 263103 (2007).
[15]W. Becker, *Advanced Time-Correlated Single Photon Counting Techniques* (Springer, 2005).

[16]L. Y. Karachinsky, S. Pellegrini, G. S. Buller, A. S. Shkolnik, N. Yu. Gordeev, V. P. Evtikhiev, and V. B. Novikov, Appl. Phys. Lett. **84**, 7 (2004).
[17]M. Sun, P. J. Simmonds, R. B. Laghumavarapu, A. Lin, C. J. Reyner, H. S. Duan, B. Liang, and D. L. Huffaker, Appl. Phys. Lett. **102**, 023107 (2013).
[18]F. Hatami, M. Grundmann, N. N. Ledentsov, F. Heinrichsdorff, R. Heitz, J. Böhrer, D. Bimberg, S. S. Ruvimov, P. Werner, V. M. Ustinov, P. S. Kop'ev, and Zh. I. Alferov, Phys. Rev. B **57**, 4635 (1998).
[19]P. D. Hodgson, R. J. Young, M. A. Kamarudin, P. J. Carrington, A. Krier, Q. D. Zhuang, E. P. Smakman, P. M. Koenraad, and M. Hayne, J. Appl. Phys. **114**, 073519 (2013).
[20]T. Inoue, S. Kido, K. Sasayama, T. Kita, and O. Wada, J. Appl. Phys. **108**, 063524 (2010).
[21]K. A. Sablon, J. W. Little, V. Mitin, A. Sergeev, N. Vagidov, and K. Reinhardt, Nano Lett. **11**, 2311 (2011).
[22]X. Yang, K. Wang, Y. Gu, H. Ni, X. Wang, T. Yang, and Z. Wang, Sol. Energy Mater. Sol. Cells **113**, 144 (2013).